Published in "Journal of the Physical Society of Japan 88(4): 044704, 2019"
which should be cited to refer to this work.

Possible Light-Induced Superconductivity in a Strongly Correlated Electron System

Nikolaj Bittner[1,2*], Takami Tohyama[3], Stefan Kaiser[1,4], and Dirk Manske[1]

[1]*Max-Planck-Institut für Festkörperforschung, D-70569 Stuttgart, Germany*
[2]*Department of Physics, University of Fribourg, 1700 Fribourg, Switzerland*
[3]*Department of Applied Physics, Tokyo University of Science, Katsushika, Tokyo 125-8585, Japan*
[4]*4th Physics Institute, University of Stuttgart, D-70569 Stuttgart, Germany*

Using a nonequilibrium implementation of the Lanczos-based exact diagonalisation technique we study the possibility of the light-induced superconducting phase coherence in a solid state system after an ultrafast optical excitation. In particular, we investigate the buildup of superconducting correlations by calculating an exact time-dependent wave function reflecting the properties of the system in non-equilibrium and the corresponding transient response functions. Within our picture we identify a possible transient Meissner effect after dynamical quenching of the non-superconducting wavefunction and extract a characteristic superfluid density that we compare to experimental data. Finally, we find that the stability of the induced superconducting state depends crucially on the nature of the excitation quench: namely, a pure interaction quench induces a long-lived superconducting state, whereas a phase quench leads to a short-lived transient superconductor.

1. Introduction

Recent developments of ultrashort laser pulses allow for optical control of the complex matter on picosecond time-scales. Intriguing experiments at mid-IR and THz frequency ranges reported controlling non-equilibrium superconductivity:[1–7] Tailored excitation pulses tuned resonantly to specific phonon modes have been shown to induce transient superconducting states far above the equilibrium transition temperature (T_c), which goes beyond the typical photo-doping experiments.[8,9] On the one hand, superconductivity could emerge after the suppression of a competing order. Here, the key experiment was performed via phonon pumping on 1/8 doped $La_{1.675}Eu_{0.2}Sr_{0.125}CuO_4$,[1,2] where superconductivity is fully suppressed due to the appearance of a competing stripe order stabilized by lattice distortion. Melting competing stripes with a light pulse allows for the reappearance[1,2] and enhancement[10,11] of the superconductivity. This picture was also supported by theoretical investigations,[12,13] where the *existing* superconductivity was enhanced after suppressing competing orders by optical pulses. However, most intriguing are experiments that really *induce* superconducting coherence into the electron system. That allows stabilizing superconducting states far above T_c;[3–6] Most prominent in $YBa_2Cu_3O_x$ (YBCO) that was possible throughout the pseudogap phase. Key to these experiments is the resonant pumping of the c-axis infrared-active CuO mode, which basically modulates the apical oxygen displacement from the CuO planes, leading to a redistribution of the interlayer coherence between the planes;[4] Although the evidence for the competing order of the incommensurate charge-density wave (CDW) in YBCO was found,[14] the temperature and time-dependent measurements rule out its melting as a key element of inducing superconductivity. A leading idea emphasizing the role of phonon pumping is based on the displacement of the lattice structure through non-linear phononics.[15,16] This transient structure frozen at maximum lattice displacement suggests an enhanced superconducting coupling strength.[17] However, comparing with theoretical expectations the transient displacement and therefore impact of this effect seems rather small to explain the observed enhanced T_c. Explanations going beyond the structural dynamics are focusing on the amplification of the *existing* electron pairing either by changing of microscopic parameters responsible for superconductivity,[18] by parametric cooling[19] or by phononic squeezing.[20–24] Though, none of them describe the possibility to induce superconducting coherence. An important experimental aspect, which was so far disregarded, is the possibility of the modulated effective interactions after optical excitation.[25] The significance of such modulations was experimentally shown on one-dimensional (1D) organic molecules,[26,27] where a controlled change in Coulomb interaction U was achieved, and most spectacular is discussed as a key element for possible light-induced superconductivity in K-doped C_{60}.[6,28,29] In the latter case, a transient superconducting state was observed after a tailored optical pulse, which modulates the local charge density. However, the understanding of the underlying microscopic mechanism in nonequilibrium is still missing.

Following that view, we propose here a general concept to induce nonequilibrium electronic phase coherence after an optical excitation (see Fig. 1) by emphasizing the role of modulated correlations U/t_h. In particular, we show the possibility of light-induced superconducting coherence following two basic concepts: pulse stimulated changes in the interaction strength of the electron system (e.g., on-site U) and modification of the electron hopping $t_h \exp(iA(t))$ by the time-dependent vector potential $A(t)$ of the light field. To capture the essential physics we simulate an electron system in nonequilibrium by the extended Hubbard model (EHM) with an additional next neighbor interaction V in 1D at half-filling[30–32] described by the time-dependent Hamiltonian:

$$\begin{aligned}\hat{H}(t) = &-t_h \sum_{i\sigma} (e^{iA(t)} \hat{c}^\dagger_{i,\sigma} \hat{c}_{i+1,\sigma} + \text{H.c.}) \\ &+ [U + \Delta U \Theta(t)] \sum_i \left(\hat{n}_{i\uparrow} - \frac{1}{2}\right)\left(\hat{n}_{i\downarrow} - \frac{1}{2}\right) \\ &+ [V + \Delta V \Theta(t)] \sum_i (\hat{n}_i - 1)(\hat{n}_{i+1} - 1), \end{aligned} \tag{1}$$

where $\hat{c}^\dagger_{i,\sigma}$ ($\hat{c}_{i,\sigma}$) creates (annihilates) an electron with spin $\sigma = \uparrow, \downarrow$ at site i and $\hat{n}_i = \hat{n}_{i\uparrow} + \hat{n}_{i\downarrow}$ denotes density operator

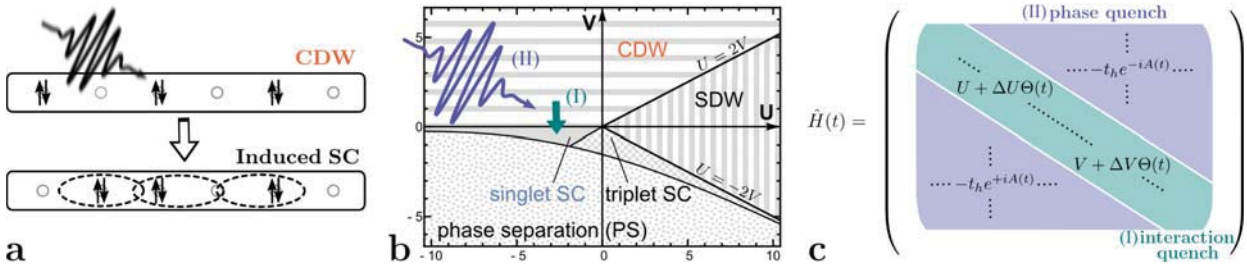

Fig. 1. (Color online) (a) Inducing phase coherence with an optical pulse. Here, spatial distribution of electrons on a lattice before and after pulse corresponds to CDW and singlet SC, respectively. (b) Illustration of the equilibrium phase diagram for the 1D EHM at half filling ($T = 0$) with U and V being the strength of the on-site and nearest neighbor interaction from Eq. (1), respectively. Each shaded region corresponds to a particular phase from EHM. The nonequilibrium transition between phases is initiated by an optical pulse following two scenarios: (I) an interaction quench or (II) a phase quench. (c) Illustration of the time-dependent Hamilton-Matrix. While after interaction quench the diagonal part of the Hamiltonian (green) is changed, phase quench modifies its off-diagonal part (blue).

with $\hat{n}_{i\sigma} = \hat{c}^{\dagger}_{i,\sigma}\hat{c}_{i,\sigma}$. Before the excitation ($t < 0$), we prepare the system in the equilibrium ground state (GS) of the CDW [see Fig. 1(a)]. Then, at around $t = 0$ the laser pulse hits, which leads to either (I) abrupt changing interaction parameters on the diagonal of the Hamiltonian (1) [green part in Figs. 1(b) and 1(c)] or (II) to a modification of the hopping by the time-dependent vector potential $A(t)$ of the light field on its off-diagonals [blue part in Figs. 1(b) and 1(c)]. We note that these excitations are tailored to dominantly change the effective correlation in case (I) (as also shown for the same system by DMRG calculations[33]) and to an effective transfer of the pulse energy to electrons in case (II).[34] Hence, one drives the system out of equilibrium and can induce a transient superconducting state [Fig. 1(a)].

2. Method

In case (I) one deals with the quench protocol,[35] where at $t = 0$ the interaction parameters U and V are abruptly changed by ΔU and ΔV. Recently this type of quenching was experimentally realized in 1D organic molecules.[26,27] The situation (II) represents an excitation with a light pulse of finite time duration. The pulse is included into the Hamiltonian by means of the Peierls substitution and is modelled by a time-dependent vector potential $A(t) = A_0 e^{-t^2/2\tau^2}\cos(\omega_{\text{pump}}t)$, with the amplitude A_0, the frequency ω_{pump}, and the full width at half maximum τ. The temporal evolution of the system obeys the Schrödinger equation, which we numerically solve by employing at each time step $t + \delta t$ Lanczos method generating a tridiagonal matrix with the eigenvectors $|\phi_l\rangle$ and corresponding eigenvalues ϵ_l. These results are subsequently used to approximate the time-dependent wave function:[34]

$$|\psi(t+\delta t)\rangle \approx e^{-i\hat{H}(t)\delta t}|\psi(t)\rangle \approx \sum_{l=1}^{M} e^{-i\epsilon_l \delta t}|\phi_l\rangle\langle\phi_l|\psi(t)\rangle. \quad (2)$$

Based on the knowledge of $|\psi(t)\rangle$ we calculate the correlation functions as well as the optical conductivity, which are good quantities to examine a contrast between two neighboring CDW and superconducting (SC) phases. The temporal evolution of the charge order can be traced by the time-dependent density–density correlation function:

$$C(j,t) = \frac{1}{L}\sum_{l=0}^{L-1}\langle\psi(t)|\hat{n}_{l+j}\hat{n}_l|\psi(t)\rangle, \quad (3)$$

at lattice site j with lattice size L. To investigate the dynamics of the singlet superconducting correlations we introduce the on-site correlation function:

$$P_1(j,t) = \frac{1}{L}\sum_{l=0}^{L-1}\langle\psi(t)|\hat{c}^{\dagger}_{l+j\downarrow}\hat{c}^{\dagger}_{l+j\uparrow}\hat{c}_{l\uparrow}\hat{c}_{l\downarrow}|\psi(t)\rangle. \quad (4)$$

We calculate the optical pump–probe conductivity $\sigma(\Delta t, \omega)$ by using an additional weak probe pulse described by $A_{\text{pr}}(\Delta t, t)$ at time delay Δt.[36,37] For a given pump we then sequentially calculate the time-dependent current density without and with the probe pulse. The difference in both results gives the current density $j_{\text{pr}}(\Delta t, t)$ induced by the probing excitation. Finally, the optical conductivity is calculated from the Fourier transformation of $j_{\text{pr}}(\Delta t, t)$ and the $A_{\text{pr}}(\Delta t, t)$ with respect to t:

$$\sigma(\Delta t, \omega) = \frac{j_{\text{pr}}(\Delta t, \omega)}{i(\omega + i\eta)LA_{\text{pr}}(\Delta t, \omega)}. \quad (5)$$

For the broadening of the spectral lines, we added artificially a small number $\eta = 1/L$.

For the numerical calculations, we use unless otherwise specified a 10-site lattice with periodic boundary conditions and set the hopping parameter $t_h = 1$. Further, we measure the energy and time in units t_h and t_h^{-1}, respectively. For the Lanczos method, we take $M = 40$ iterations and the time interval $\delta t = 0.01$.

3. Results

3.1 Induced phase coherence due to interaction quench

The light induced abrupt change in the interaction strength of the electron system leads to the modification in its eigenstates and, in turn, to the redistribution of the electrons on a lattice. For visualization, we have calculated the excitation spectrum of the system in nonequilibrium and compared it with its equilibrium counterparts before and after quenching [see Fig. 2(a)]. At $t < 0$ we prepare the system in the equilibrium GS of the CDW with $U = -4$, $V = 0.25$ and switch abruptly at $t = 0$ the interaction parameter V into the superconducting region with $V = -0.25$ (green part in Fig. 1). Analyzing the excitation spectrum in nonequilibrium (black line) in Fig. 2(a) we can draw some important conclusions. First of all, there are no peaks in the spectrum, which could be identified with the equilibrium CDW phase (red area). Moreover, the most intensive peaks in the spectrum correspond to the low-energy excited states in the

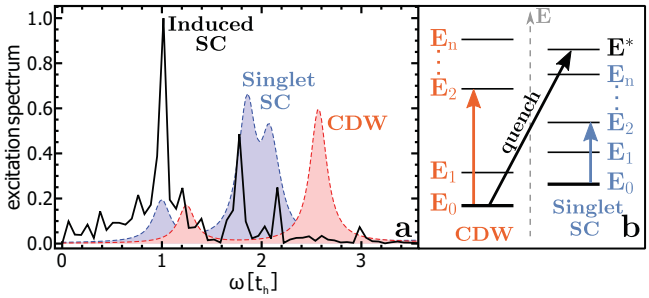

Fig. 2. (Color online) (a) Excitation spectrum of the system in nonequilibrium (black solid line) compared with the spectra in equilibrium SC phase (blue region) and equilibrium CDW phase (red region). (b) Schematic illustration of the interaction quench together with excitation processes in SC and CDW phases. Black bars represent energy levels E_n in both phases. A nonequilibrium state is indicated by E^*.

equilibrium SC phase (blue area). Finally, since the interaction quench is a nonadiabatic process, the system does not appear in the GS of the singlet SC phase after quenching, but in some nonequilibrium state E^*. Physically that means, that after quenching the system goes directly into a nonequilibrum state in the SC phase and the CDW is fully suppressed, as schematically summarized in Fig. 2(b). Moreover, this tailored excitation dominantly leads to an effective transfer of the applied energy to the changes of the correlation in the system, rather than to its heating.[33] As shown below, the SC correlations in nonequilibrium are almost immediately induced after quenching (within few t_h^{-1}). Otherwise, the system would end up in a thermal state with a high effective temperature, where the superconducting correlations are not expected. Note that also experimentally no change of the kinetic energy was observed during the interaction quench in 1D organic molecules.[26]

To show how superconducting signatures emerges after the interaction quench with time, we calculate the correlation functions and more significantly the experimentally relevant time-dependent optical conductivity $\sigma(\Delta t, \omega)$ [see Eq. (5)]. First, we plot in Figs. 3(a) and 3(b) the time-dependent density–density $C(j,t)$ and on-site $P_1(j,t)$ correlation functions defined in Eqs. (3) and (4), respectively. Clearly, the CDW state prepared at $t < 0$ and showing characteristic "zigzag" structure in Fig. 3(a) is strongly suppressed after quenching. At the same time, $P_1(j,t)$ presented in Fig. 3(b) shows strong enhancement of the superconducting correlations in nonequilibrium. Moreover, a direct comparison of $P_1(j,t)$ in nonequilibrium with the result for the equilibrium superconducting GS (blue dashed line) reveals a quite good agreement. Finally, we focus on the optical conductivity. Superconductivity is identified in the complex $\sigma(\Delta t, \omega)$ as follows: Due to the perfect diamagnetic response of a superconductor, the imaginary part $\sigma_2(\Delta t, \omega)$ diverges with a characteristic Landau $1/\omega$-behavior for $\omega \to 0$ indicating the Meissner effect. The perfect conductivity leads in the real part $\sigma_1(\Delta t, \omega)$ to the opening of a superconducting gap in the optical conductivity and a transfer of spectral weight into the zero frequency δ-peak. In Fig. 3(c) we show $\sigma_2(\Delta t, \omega)$ and $\sigma_1(\Delta t, \omega)$ (inset) calculated in the equilibrium superconducting state (blue dashed line) and after quenching (solid lines). Clearly, after quenching $\sigma_2(\Delta t, \omega)$ shows the disappearance of the CDW response visible as the clear spectral feature $\omega \approx 1.8$ in the equilibrium spectra (red solid line) and the appearance of a clear inductive response with a superconducting-like $1/\omega$ behavior in the transient spectra (blue solid lines). That indicates the emergence of the superconducting correlations via the Meissner effect. In order to characterize the induced superfluid density, we calculated $\langle \omega \Delta\sigma_2 \rangle$.[38] Here, we found a sudden enhancement of its value after the quench with subsequent oscillations. Moreover, the transient value of $\langle \omega \Delta\sigma_2 \rangle$ is comparable with its equilibrium counterpart for the superconducting phase, if the temperature due to the quench is taken into account. Equivalent indications were also found in the temporal evolution of $\sigma_1(\Delta t, \omega)$, where the spectral weight of the low energy peak at $\omega \approx 1.8$ corresponding to the equilibrium CDW state is shifted after quenching into the low-energy

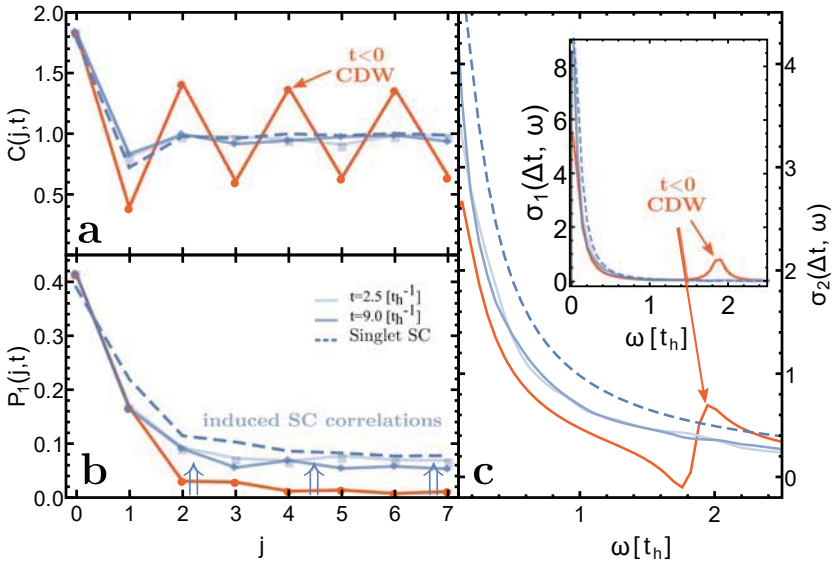

Fig. 3. (Color online) Time-dependent (a) density–density and (b) on-site correlation functions for 14-site lattice obtained for the interaction quench ($U = -4$, $V = 0.25$, $\Delta V = -0.5$). Results for equilibrium SC phase are indicated by blue dashed lines. (c) The calculated corresponding imaginary optical conductivity $\sigma_2(\Delta t, \omega)$ at times: $\Delta t < 0$ (red solid line), $\Delta t = 2.5$ (light blue solid line), and $\Delta t = 9$ (blue solid line). Its real part $\sigma_1(\Delta t, \omega)$ is shown in inset.

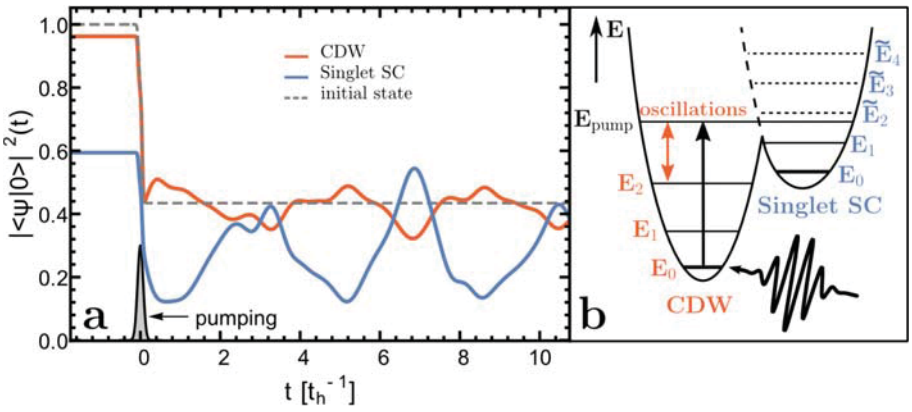

Fig. 4. (Color online) (a) Time-dependent overlap function $|\langle\psi(t)|0\rangle|^2$ for: $U = -3$ and $V = 0.7$ (CDW), -0.5 (Singlet SC), and 0.5 (initial state). The pulse has a Gaussian shape with parameters: $A_0 = 5$, $\omega = 2.38$, $\tau = 0.05$ and is indicated by the black region around $t = 0$. (b) Illustration of the excitation of a system by a strong light pulse.

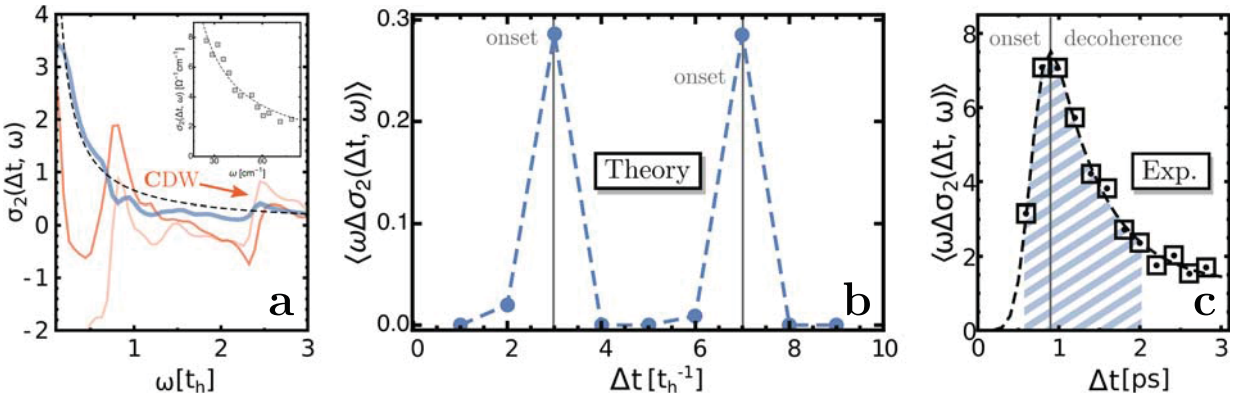

Fig. 5. (Color online) (a) Time-dependent imaginary conductivity $\sigma_2(\Delta t, \omega)$. Theoretically obtained results at different time delays are presented by the solid lines: $\Delta t = 1$ (light red), $\Delta t = 2$ (red), and $\Delta t = 3$ (blue). The $1/\omega$-fit for the latter case is shown by the dashed line. Experimentally measured data for YBCO with $x = 6.45$ at $T = 100$ K and $\Delta t = 0.8$ ps is illustrated by the black squares in inset. (b) Theoretically calculated for the Hubbard model and (c) experimentally measured[5] for YBCO with $x = 6.45$ at $T = 100$ K transient value of $\langle\omega\Delta\sigma_2(\Delta t, \omega)\rangle$ for different time delays Δt. The gray solid lines separate onset and decoherence areas on figures.

peak at $\omega \approx 0$.[39] We note that the finite low-frequency tail in the equilibrium CDW state is an artefact of the finite-size calculation. In the induced non-equilibrium case all spectral weight that gets transferred into the low-frequency peak is interpreted as a spectral weight that forms the transient δ-peak of the superfluid. Note that due to the finite size of our model system all this weight is below the low frequency cut off frequency. This weight tracks the equilibrium superconducting δ-peak [shown as blue dashed line in the inset of Fig. 3(c)] that also appears with a finite width in our finite size model.

3.2 *Realistic phase quench and comparison with experiment*

Now, we investigate the second important case, where a light pulse modifies the electron hopping with the possibility to induce phase coherence between the electron pairs on the lattice. Since it is technically impossible to calculate the superconducting order parameter within our method, we use some related quantities for our studies of the induced superconducting correlations. First, we calculate the projection of the time-dependent wave function $|\psi(t)\rangle$ from Eq. (2) to different ground states $|0\rangle$ [see Fig. 4(a)]. The system is initially prepared in the GS with $U = -3$, $V = 0.5$ (CDW phase) and at $t = 0$ gets exposed to the light field with a finite width (blue part in Fig. 1). The central frequency of the pulse is resonantly tuned to the first low-energy excited state in the CDW phase to guarantee an effective transfer of the pulse energy to the electrons.[34] The pulse duration is set to $\tau = 0.05$ allowing to reach simultaneously different excited states of the system. Clearly, after pumping the CDW component in $|\psi(t)\rangle$ is only partially suppressed (red solid line), whereas the projection to the superconducting GS (blue solid line) shows a temporal enhancement in the overlap function $|\langle\psi(t)|0\rangle|^2$. One should also note that the overlap of the initial CDW state with the superconducting one before the quench is nonzero and indicates non-orthogonal ground states. However, at $t \approx 7$ the overlap with the superconducting GS is even larger than with the initial state (gray dashed line). This might indicate an excitation of the system to some joint state of the CDW and SC, as illustrated in Fig. 4(b). The interpretation of a dynamical coexistence of both phases is also supported by the excitation spectrum and correlation functions.[40] Note that owing to the resonant driving of the system the pulse energy goes effectively to the change of correlations. Otherwise, the corresponding thermal state would have a rather high effective temperature, where the buildup of the superconducting correlations is not expected.

Next, to explore the temporal dynamics of this joint state and to find further fingerprints of the superconducting phase coherence, we calculate the time-dependent optical conductivity (see Fig. 5). In Fig. 5(a) we show $\sigma_2(\Delta t, \omega)$,[41] where we observe a reduction of the equilibrium low-energy CDW response at both $t = 1$ (light red line) and $t = 2$ (red line) with the appearance of an in-gap state at $\omega \approx 0.7$. Subsequently, at $t = 3$ (blue line) the response from CDW has disappeared and the data can be fitted to a $1/\omega$ dependence (black dashed line). This characteristic Landau $1/\omega$-like behavior we attribute as the diamagnetic response emerging from the superconducting correlation due to the Meissner effect. We note that a $1/\omega$ behavior is a generic characteristics found throughout induced superconductors.[1,3,6,10] For illustration, we plot in the inset to Fig. 5 the induced inductive response exemplary for the cuprate YBCO with $x = 6.45$ under phonon pumping[5] (open black squares). These experimental data shows an induced $1/\omega$ behaviour and was also interpreted as an induced inductive response of a transient Meissner effect. Finally, to characterize the induced superfluid density we calculate $\omega\Delta\sigma_2(\Delta t, \omega)$ by fitting the $1/\omega$ divergence at low frequencies for each spectrum. Figure 5(b) shows the extracted transient superfluid density as a function of time delay Δt. Clearly, pumping the system leads to an induction of a finite superfluid density with an onset between $\Delta t = 1$ to 3. On the other hand, the dynamical coexistence of the CDW and superconducting excitations leads to the characteristic oscillating behavior discussed above. This is also seen in the reappearing onset in $\omega\Delta\sigma_2(\Delta t, \omega)$ between $\Delta t = 5$ to 7. Hence, the transient character of $|\psi(t)\rangle$ [see Fig. 4(a)] describes a periodic decoherence and therefore leads to a short-lived transient superconducting state. While the onset behaviour of the above mentioned cuprate YBCO with $x = 6.45$ [see Fig. 5(c)] shows clear similarities to our model calculations the stability of the light-induced state has to be interpreted differently: The short-lived character of the experimentally induced state is due to dephasing of the light-induced superfluid by the loss of long-range coherence into several decay and dephasing channels,[5] while in our model calculation the short-lived character is due to the oscillatory behaviour between SC and CDW order in the model system without decay channels.

4. Conclusion

In the present paper, we have studied the possibility that tailored light pulses that modulate correlations induce superconducting phase coherence in transient nonequilibrium states. The nonequilibrium dynamics in a solid state system we simulated using time-dependent Lanczos-based exact diagonalization technique.

Calculating the transient ac-optical conductivity we found transfer of a spectral weight into the zero frequency peak in σ_1 indicating an increase of the conductivity of the system. More importantly, we observed $1/\omega$ divergence at $\omega \to 0$ in imaginary conductivity σ_2 within the low-frequency cut-off given by the dimensionality of our system. In contrast to a conventional conductor, where one finds a Drude peak in σ_1 and a broad peak in σ_2 defined by the scattering rate, these signatures indicate a superconducting state. However, the optical properties of a superconductor cannot be distinguished from that of a perfect conductor. This is of particular importance since the electron system that we consider here is dissipationless. In this case, the $1/\omega$ behavior in σ_2 would not be a unique identification for the Meissner-effect. Therefore, to exclude the possibility of photo-doping the system, where the photo-doped electrons would lead to a metallic response, we calculated the double occupancy function:[42] here we find the existence of paired electrons in the driven state, which is indicative for a superconductor. A metallic response would show instead single occupancies. We note that a similar dependence of the double occupancy function was observed for the Falicov–Kimball model and was attributed to the melting of CDW order.[43] However, the response of the CDW in our case is almost completely suppressed in the nonequilibrium state. Moreover, both in the correlation functions, excitation spectra and in the transient wavefunction we find further fingerprints for the transient superconducting response in the light-induced state. Hence, our comprehensive picture allows interpreting the $1/\omega$ inductive response as a transient Meissner effect, since it clearly emerges from the induced superconducting correlations and excitations. The behavior of σ_2 allows us extracting the induced superfluid densities and a comparison with experimental quantities. Based on the quench processes the induced nonequilibrium states show distinct different transient behaviors. While for a pure interaction quench a long-lived superconducting state can be induced, for a phase quench a short-lived transient superconducting state emerges.

Acknowledgments The authors are grateful to A. Schnyder, A. Cavalleri, Y. Murakami, and H. Krull for helpful discussions. N.B. thanks the YITP in Kyoto, Japan for its hospitality. S.K. acknowledges support from the Ministerium für Wissenschaft, Forschung und Kunst Baden-Württemberg through the Juniorprofessuren-Programm and support from the Daimler und Benz Stiftung.

*Corresponding author. E-mail: nikolaj.bittner@unifr.ch

1) D. Fausti, R. I. Tobey, N. Dean, S. Kaiser, A. Dienst, M. C. Hoffmann, S. Pyon, T. Takayama, H. Takagi, and A. Cavalleri, Science **331**, 189 (2011).
2) C. R. Hunt, D. Nicoletti, S. Kaiser, T. Takayama, H. Takagi, and A. Cavalleri, Phys. Rev. B **91**, 020505 (2015).
3) S. Kaiser, C. R. Hunt, D. Nicoletti, W. Hu, I. Gierz, H. Y. Liu, M. Le Tacon, T. Loew, D. Haug, B. Keimer, and A. Cavalleri, Phys. Rev. B **89**, 184516 (2014).
4) W. Hu, S. Kaiser, D. Nicoletti, C. R. Hunt, I. Gierz, M. C. Hoffmann, M. Le Tacon, T. Loew, B. Keimer, and A. Cavalleri, Nat. Mater. **13**, 705 (2014).
5) C. R. Hunt, D. Nicoletti, S. Kaiser, D. Pröpper, T. Loew, J. Porras, B. Keimer, and A. Cavalleri, Phys. Rev. B **94**, 224303 (2016).
6) M. Mitrano, A. Cantaluppi, D. Nicoletti, S. Kaiser, A. Perucchi, S. Lupi, P. Di Pietro, D. Pontiroli, M. Ricc, S. R. Clark, D. Jaksch, and A. Cavalleri, Nature **530**, 461 (2016).
7) S. Kaiser, Phys. Scr. **92**, 103001 (2017).
8) A. Pashkin, M. Porer, M. Beyer, K. W. Kim, A. Dubroka, C. Bernhard, X. Yao, Y. Dagan, R. Hackl, A. Erb, J. Demsar, R. Huber, and A. Leitenstorfer, Phys. Rev. Lett. **105**, 067001 (2010).
9) S. Dal Conte, C. Giannetti, G. Coslovich, F. Cilento, D. Bossini, T. Abebaw, F. Banfi, G. Ferrini, H. Eisaki, M. Greven, A. Damascelli, D. van der Marel, and F. Parmigiani, Science **335**, 1600 (2012).
10) D. Nicoletti, E. Casandruc, Y. Laplace, V. Khanna, C. R. Hunt, S. Kaiser, S. S. Dhesi, G. D. Gu, J. P. Hill, and A. Cavalleri, Phys. Rev. B **90**, 100503 (2014).
11) E. Casandruc, D. Nicoletti, S. Rajasekaran, Y. Laplace, V. Khanna, G. D. Gu, J. P. Hill, and A. Cavalleri, Phys. Rev. B **91**, 174502 (2015).
12) A. A. Patel and A. Eberlein, Phys. Rev. B **93**, 195139 (2016).
13) Z. M. Raines, V. Stanev, and V. M. Galitski, Phys. Rev. B **91**, 184506

(2015).
14) M. Först, A. Frano, S. Kaiser, R. Mankowsky, C. R. Hunt, J. J. Turner, G. L. Dakovski, M. P. Minitti, J. Robinson, T. Loew, M. Le Tacon, B. Keimer, J. P. Hill, A. Cavalleri, and S. S. Dhesi, Phys. Rev. B **90**, 184514 (2014).
15) M. Först, C. Manzoni, S. Kaiser, Y. Tomioka, Y. Tokura, R. Merlin, and A. Cavalleri, Nat. Phys. **7**, 854 (2011).
16) R. Mankowsky, A. Subedi, M. Forst, S. O. Mariager, M. Chollet, H. T. Lemke, J. S. Robinson, J. M. Glownia, M. P. Minitti, A. Frano, M. Fechner, N. A. Spaldin, T. Loew, B. Keimer, A. Georges, and A. Cavalleri, Nature **516**, 71 (2014).
17) A. Subedi, A. Cavalleri, and A. Georges, Phys. Rev. B **89**, 220301 (2014).
18) M. A. Sentef, A. F. Kemper, A. Georges, and C. Kollath, Phys. Rev. B **93**, 144506 (2016).
19) S. J. Denny, S. R. Clark, Y. Laplace, A. Cavalleri, and D. Jaksch, Phys. Rev. Lett. **114**, 137001 (2015).
20) M. Knap, M. Babadi, G. Refael, I. Martin, and E. Demler, Phys. Rev. B **94**, 214504 (2016).
21) M. Babadi, M. Knap, I. Martin, G. Refael, and E. Demler, Phys. Rev. B **96**, 014512 (2017).
22) Y. Murakami, N. Tsuji, M. Eckstein, and P. Werner, Phys. Rev. B **96**, 045125 (2017).
23) D. M. Kennes, E. Y. Wilner, D. R. Reichman, and A. J. Millis, Nat. Phys. **13**, 479 (2017).
24) M. A. Sentef, Phys. Rev. B **95**, 205111 (2017).
25) E. Pomarico, M. Mitrano, H. Bromberger, M. A. Sentef, A. Al-Temimy, C. Coletti, A. Stöhr, S. Link, U. Starke, C. Cacho, R. Chapman, E. Springate, A. Cavalleri, and I. Gierz, Phys. Rev. B **95**, 024304 (2017).
26) S. Kaiser, S. R. Clark, D. Nicoletti, G. Cotugno, R. I. Tobey, N. Dean, S. Lupi, H. Okamoto, T. Hasegawa, D. Jaksch, and A. Cavalleri, Sci. Rep. **4**, 3823 (2014).
27) R. Singla, G. Cotugno, S. Kaiser, M. Först, M. Mitrano, H. Y. Liu, A. Cartella, C. Manzoni, H. Okamoto, T. Hasegawa, S. R. Clark, D. Jaksch, and A. Cavalleri, Phys. Rev. Lett. **115**, 187401 (2015).
28) M. Kim, Y. Nomura, M. Ferrero, P. Seth, O. Parcollet, and A. Georges, Phys. Rev. B **94**, 155152 (2016).
29) G. Mazza and A. Georges, Phys. Rev. B **96**, 064515 (2017).
30) J. Sólyom, Adv. Phys. **28**, 201 (1979).
31) J. Voit, Phys. Rev. B **45**, 4027 (1992).
32) J. Voit, Rep. Prog. Phys. **58**, 977 (1995).
33) S. Paeckel, B. Fauseweh, T. Köhler, S. Manmana, and D. Manske, to be published.
34) H. Lu, S. Sota, H. Matsueda, J. Bonča, and T. Tohyama, Phys. Rev. Lett. **109**, 197401 (2012).
35) M. Eckstein, M. Kollar, and P. Werner, Phys. Rev. B **81**, 115131 (2010).
36) C. Shao, T. Tohyama, H.-G. Luo, and H. Lu, Phys. Rev. B **93**, 195144 (2016).
37) Z. Lenarčič, D. Golež, J. Bonča, and P. Prelovšek, Phys. Rev. B **89**, 125123 (2014).
38) (Supplemental Material) The details to the temporal dynamics of $\omega\Delta\sigma_2$ is provided online.
39) (Supplemental Material) The details of the dynamics of the low-energy peak at $\omega = 0$ is provided online.
40) (Supplemental Material) The details to the excitation spectrum and correlation functions is provided online.
41) (Supplemental Material) Real part of the optical conductivity is provided online.
42) (Supplemental Material) The details to the double occupancy function is provided online.
43) J. K. Freericks, O. P. Matveev, W. Shen, A. M. Shvaika, and T. P. Devereaux, Phys. Scr. **92**, 034007 (2017).